IEEE Access
Multidisciplinary | Rapid Review | Open Access Journal

Received November 20, 2017, accepted December 15, 2017, date of publication December 22, 2017,
date of current version February 14, 2018.

Digital Object Identifier 10.1109/ACCESS.2017.2786246

Evaluation of Electromagnetic Fields Induced by Wake of an Undersea-Moving Slender Body

ZHIHUA XU, (Student Member, IEEE), CHANGPING DU, (Student Member, IEEE), AND MINGYAO XIA, (Senior Member, IEEE)
School of Electronics Engineering and Computer Science, Peking University, Beijing 100871, China
Corresponding author: Mingyao Xia (myxia@pku.edu.cn)

This work was supported by the NSFC under Project 61531001.

ABSTRACT This paper presents the procedure for evaluating the electromagnetic field induced by the wake of an undersea-moving slender body. The slender body is considered equivalent to a pair of Havelock point sources that can generate wake flow fields. The electric current generated in the seawater is calculated by means of the moving conductive seawater that cuts the earth's magnetic field. The electromagnetic fields in the air and in the seawater are then determined by solving the Maxwell equations with appropriate boundary conditions. The induced electromagnetic fields include two parts: One is the attenuating oscillation that can be ascribed to the free surface Kelvin wake, and the other is the bipolar pulse that can be ascribed to the localized volume wake. Near the sea surface, the magnitude of the former is typically a few hundred pico-tesla, while that of the latter could be greater by ten times.

INDEX TERMS Electromagnetic fields, moving seawater, undersea body, wake.

I. INTRODUCTION

The movement of conductive seawater in the Earth's magnetic field is just like that of the mental conductor in the magnetic field, which produces inductive electromagnetic fields. This phenomenon was predicted by Faraday in 1832 [1] and experimentally confirmed by Young *et al.* in 1920 [2]. Since the 1960s, extensive investigations were conducted on the electromagnetic fields relating to moving seawater, including wind waves and swells [3]–[6], internal waves [7]–[9], tidal or oceanic currents [10], [11], tsunami waves [12], and wakes of ships or submarines [13]–[18]. In addition to the theoretical analyses, instrument developments and in-site measurements have also been reported [7], [19]–[21]. These studies show that the magnitude of the induced magnetic field is typically of the order of a fraction of one nano-Tesla (nT), which may be regarded as a big value, because, nowadays, the precision of commercial optical pumping magnetometer is typically several pico-Teslas (pT). While the induced electromagnetic fields provide useful information for oceanographic research, the noises they generate are detrimental to marine electromagnetic prospecting, such as the controllable source electromagnetic sounding technique [22], [23]. In the years to come, investigation of electromagnetic fields produced by moving seawater is expected to become an essential part of marine electromagnetics and applications.

The free surface Kelvin wake, generated by a ship or a submarine, can spread over several kilometers and sustain more than ten minutes. It can be considered a steady signature for probing the targets. Sensing the magnetic anomaly fields produced by wakes has been proposed as a potential method for detecting ships and submarines [13], [14]. Evaluation of the electromagnetic fields, produced by the wakes, has thus started attracting increased attention. In 1994, Madurasinghe *et al.* presented their simulation results, for the first time, which hold for a surface ship [15], as well as a moving body submerged in the ocean of infinite depth [16]. The infinite depth ocean model was also employed by Zhu and Xia [17], Xu *et al.*[18]. However, their works suffer from one common drawback: In their works, they considered only the surface Kelvin wake or far flow field and totally ignored the volume wake or near flow field. Though the surface wake can span over several kilometers, its undulations diminish as the submerged depth increases. The volume wake, on the other hand, is usually much stronger than the surface wake and changes little as the submerged depth increases. Therefore, taking the volume wake into account is necessary for a complete evaluation of the produced electromagnetic fields, and that is precisely the purpose of this paper.

The remainder of this paper is organized as follows. Section II outlines the modeling of wake produced by an

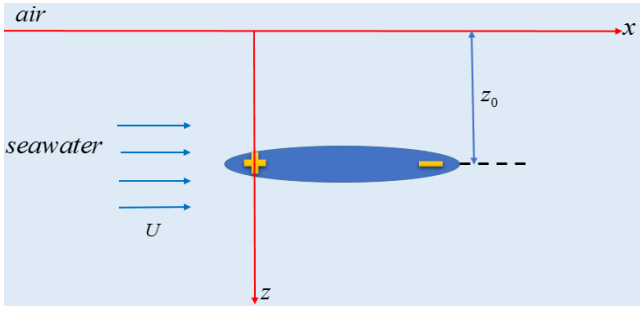

FIGURE 1. Illustration of a slender body of volume V, moving undersea with speed U at depth z_0.

undersea-moving slender body. Section III derives the solutions for the electromagnetic fields induced by the wake. Section IV presents simulation results and discussions. Finally, Section V presents the conclusions drawn from this study.

II. WAKE OF AN UNDERSEA MOVING SLENDER BODY

It is assumed that a slender body is moving under the sea surface with speed U, at depth z_0 (see Figure 1). Its x axis is pointing towards its rear, z axis towards its bottom, and y axis is so selected that xyz forms a right-hand system. The seawater is taken to be incompressible; besides, the jet-flow by the propeller is not considered at the moment. For incompressible seawater, the velocity field $\boldsymbol{v}$ of the wake can be expressed by potential φ as $\mathbf{v} = -\nabla\varphi$. The potential function φ should satisfy four equations and boundary conditions [18]: (i) the Laplace equation, (ii) the normal component of the velocity vanishes on the body surface, (iii) the kinematics equation at the air-seawater interface, and (iv) the kinetics equation at the air-seawater interface. The kinematics and kinetics equations are nonlinear, which render obtaining a completely analytical solution for φ impossible. However, they can be linearized, if the surface undulations of the wake are weak. Once linearized, it can be shown by the hydrodynamics theory [24] that the water flow or the wake produced by a slender body can be equivalent to that produced by a pair of Havelock point sources, separated by L and having strength $\pm UV/L$, where V is the volume of the body. A point source of unit strength that satisfies the following equation and boundary condition is called the unit Havelock point source:

$$\begin{cases} \nabla^2 G = -\delta(x)\delta(y)\delta(z - z_0) \\ [k_0 G_z - G_{xx} - \gamma G_x]_{z=0} = 0 \end{cases} \tag{1}$$

where $k_0 = g/U^2$ with $g = 9.81$ m/s^2 the acceleration of gravity, γ is the viscosity that will be taken to be zero later, $G_z = \partial G/\partial z$, and so forth. Therefore, the potential φ due to a pair of Havelock point sources, is

$$\varphi(x, y, z, t) = \frac{UV}{L}\left[G(x + Ut, y, z) - G(x - L + Ut, y, z)\right] \tag{2}$$

Using Fourier transform of (1) and changing the spectral integrals from Cartesian coordinate system into polar coordinate system, it is not difficult to show that the solution to (1) is

$$G(x, y, z) = \frac{1}{(2\pi)^2}\mathrm{Re}\int_{-\pi/2}^{\pi/2}\int_0^{\infty}\tilde{G}(k, \theta, z)\, e^{jk\Omega} dk d\theta \tag{3}$$

$$\tilde{G}(k, \theta, z) = e^{-k|z - z_0|} - e^{-k(z+z_0)} - \frac{2k_p}{k - (k_p + j\gamma\sec\theta)} e^{-k(z+z_0)} \tag{4}$$

with

$$k_p = k_0 \sec^2\theta \tag{5}$$

$$\Omega(x, y, \theta) = x\cos\theta + y\sin\theta. \tag{6}$$

Substituting (4) into (3), the integral, with respect to k, may be carried out in closed-form expressions, and the Green function G may be written in four parts [25], [26]. The first part is obviously the direct contribution by the source, which is expressed as

$$G_1 = \frac{1}{(2\pi)^2}\mathrm{Re}\int_{-\pi/2}^{\pi/2}\int_0^{\infty} e^{-k|z - z_0|} e^{jk\Omega} dk d\theta = \frac{1}{4\pi R_1}, \quad R_1 = \sqrt{x^2 + y^2 + (z - z_0)^2}. \tag{7}$$

The second part is the contribution from an imaginary sink above the surface, which is expressed as

$$G_2 = -\frac{1}{4\pi R_2}, \quad R_2 = \sqrt{x^2 + y^2 + (z + z_0)^2}. \tag{8}$$

The third part is the contribution by the polar point at $k = k_p + j\gamma\sec\theta$, which is a surface characteristic mode or the free surface Kelvin wake. Referring to Figure 2 for the integral routine, and using the residual theorem, we have

$$G_3 = \frac{1}{\pi}\mathrm{Im}\int_{-\pi/2}^{\pi/2} k_p e^{-k_p(z+z_0)} u(\Omega) e^{jk_p\Omega} d\theta \tag{9}$$

with

$$u(\Omega) = \begin{cases} 1, & \Omega > 0 \\ 0, & \Omega \le 0 \end{cases} \tag{10}$$

where $\gamma \to 0$ has been used. The step function $u(\Omega)$ indicates that the Kelvin wake exists only on the rear side of the moving body. The last part, the contribution of the third term of (4) after excluding the polar point contribution, may be written as

$$G_4 = \frac{1}{(2\pi)^2}\mathrm{Re}\int_{-\pi/2}^{\pi/2}\Theta(x, y, z, \theta) d\theta \tag{11}$$

with

$$\Theta = \int_0^{\infty}(1 \pm j) d\eta \left[\frac{-2k_p}{k - k_p} e^{-k(z+z_0)} e^{jk\Omega}\right]_{k=(1\pm j)\eta} \tag{12}$$

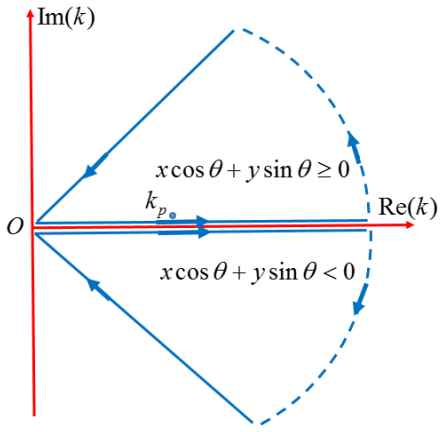

FIGURE 2. Contour integral schematic diagram.

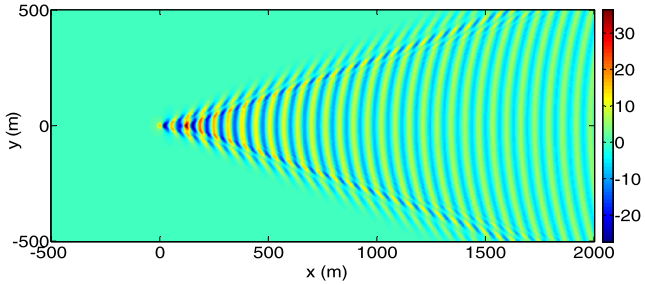

FIGURE 3. Free surface Kelvin wake pattern for $z_0 = 10$ m. The included angle between the two arms is nearly 39 degrees.

where $k = (1 + j)\eta$ applies for $\Omega > 0$ and $k = (1 - j)\eta$ for $\Omega \leq 0$. The integral of (12) may be further expressed by exponential integral function. Using the above formulae, the velocity field of the whole wake can be resolved by $\mathbf{v} = -\nabla\varphi$, and particularly, the surface wake elevation by

$$\xi(x, y) = \frac{U}{g}\left.\frac{\partial\varphi}{\partial x}\right|_{z=0}. \tag{13}$$

Two typical free surafce Kelvin wake patterns (elevation in meter) are shown in Figure 3 and Figure 4 for depth (z_0) 10 m and 50 m, respectively. A profile of the wake pattern in the *xz*-plane of Figure 4 is shown in Figure 5.

III. ELECTROMAGNETIC FIELDS INDUCED BY WAKE

We can first consider the electromagnetic field due to a unit strength Havelock point source with the Green function (3), and then obtain the total field induced by a pair of Havelock point sources by noting (2). The electric current density induced in the seawater can be fairly approximated by using

$$\begin{aligned}\mathbf{J}(x, y, z, t) &= \sigma_1\left[-\nabla G(x + Ut, y, z) \times \mathbf{F}_0\right] \\ &= -\mathrm{Im}\int_{-\pi/2}^{\pi/2}\int_0^{\infty}\left[\bar{\mathbf{K}}e^{-k|z-z_0|} - \mathbf{K}\Gamma e^{-k(z+z_0)}\right]e^{jk\tilde{\Omega}}kdkd\theta\end{aligned} \tag{14}$$

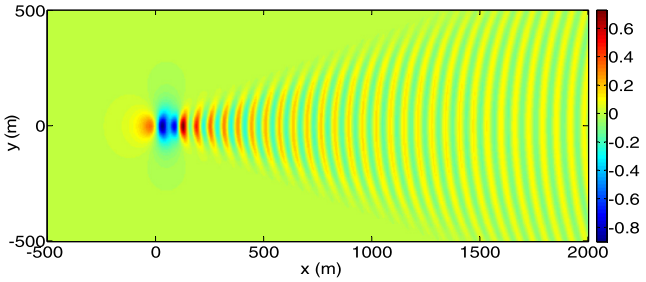

FIGURE 4. Free surface Kelvin wake pattern for $z_0 = 50$ m. The included angle of the V-shape area is also nearly 39 degrees.

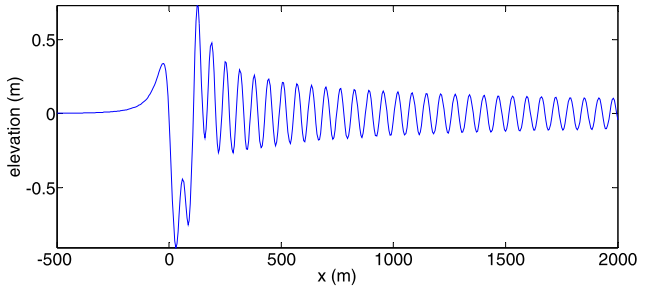

FIGURE 5. Free surface Kelvin wake profile in the xz-plane of Figure 4 for $z_0 = 50$ m.

with

$$\bar{\mathbf{K}} = \begin{cases}\mathbf{K}^*, 0 \leq z < z_0 \\ \mathbf{K}, \ z \geq z_0\end{cases} \tag{15}$$

where σ_1 is the conductivity of the seawater, $\mathbf{F}_0$ the Earth magnetic field, $\mathbf{K}^*$ the complex conjugate of $\mathbf{K}$, and

$$\Gamma = 1 + \frac{2k_p}{k - k_p} \tag{16}$$

$$\tilde{\Omega}(x, y, t, \theta) = (x + Ut)\cos\theta + y\sin\theta \tag{17}$$

$$\mathbf{K} = \frac{\sigma}{(2\pi)^2}\mathbf{F}_0 \times (\hat{h} + j\hat{z}) \tag{18}$$

$$\hat{h} = \hat{x}\cos\theta + \hat{y}\sin\theta \tag{19}$$

The induced electromagnetic fields can be acquired via the magnetic vector potential, which, in the seawater, satisfies

$$\left(\nabla^2 - \mu_0\sigma_1\frac{\partial}{\partial t} - \mu_0\varepsilon_1\frac{\partial^2}{\partial t^2}\right)\mathbf{A}_1(x, y, z, t) = -\mu_0\mathbf{J}(x, y, z, t) \tag{20}$$

A special solution to this equation is

$$\mathbf{A}_1^p(\mathbf{r}, t) = \mu_0\mathrm{Im}\int_{-\pi/2}^{\pi/2}\int_0^{\infty}\left[\bar{\mathbf{K}}f_1(z) - \mathbf{K}\Gamma f_2(z)\right]e^{jk\tilde{\Omega}}kdkd\theta \tag{21}$$

where the authors have defined

$$\omega = kU\cos\theta \tag{22}$$

$$\beta_i^2 = \omega^2\mu_0\varepsilon_i - j\omega\mu_0\sigma_i, \quad i = 0, 1 \tag{23}$$

$$\alpha_i = \sqrt{k^2 - \beta_i^2}, \quad i = 0, 1 \tag{24}$$

$$f_1(z) = \frac{e^{-k|z-z_0|} - e^{-\alpha_1|z-z_0|}}{\beta_1^2} \tag{25}$$

$$f_2(z) = \frac{e^{-k(z+z_0)} - e^{-\alpha_1(z+z_0)}}{\beta_1^2}. \tag{26}$$

The second terms in (25) and (26) are intentionally added, so that the solution (21) remains applicable even when $U\cos\theta \to 0$, i.e.,

$$\lim_{U\cos\theta\to 0} f_1(z) = -\frac{|z-z_0|}{2k} \tag{27}$$

$$\lim_{U\cos\theta\to 0} f_2(z) = -\frac{z+z_0}{2k} \tag{28}$$

The general solutions in the air and seawater may be written, respectively, as:

$$\mathbf{A}_0(\mathbf{r}, t) = \mu_0 \mathrm{Im} \int_{-\pi/2}^{\pi/2} \int_0^{\infty} \mathbf{P} f_1(0) e^{\alpha_0 z} e^{jk\tilde{\Omega}} k dk d\theta \tag{29}$$

$$\mathbf{A}_1^s(\mathbf{r}, t) = \mu_0 \mathrm{Im} \int_{-\pi/2}^{\pi/2} \int_0^{\infty} \mathbf{Q} f_1(0) e^{-\alpha_1 z} e^{jk\tilde{\Omega}} k dk d\theta \tag{30}$$

where $\mathbf{P}$ and $\mathbf{Q}$ are two constant vectors to be determined, which may be written as the tangential and normal components:

$$\mathbf{P}(k, \theta) = \mathbf{P}_t(k, \theta) + P_z(k, \theta)\hat{z} \tag{31}$$

$$\mathbf{Q}(k, \theta) = \mathbf{Q}_t(k, \theta) + Q_z(k, \theta)\hat{z} \tag{32}$$

in which $P_z(k, \theta) = \hat{z}\cdot\mathbf{P}(k, \theta)$, $\mathbf{P}_t(k, \theta) = \mathbf{P}(k, \theta) - P_z(k, \theta)\hat{z}$, and so forth.

The electric field and magnetic field are obtained from the vector potentials, which, in the spectral domain, are

$$\tilde{\mathbf{E}} = -j\omega\tilde{\mathbf{A}} + \frac{\nabla\nabla\cdot\tilde{\mathbf{A}}}{j\omega\mu\varepsilon^*} \tag{33}$$

$$\tilde{\mathbf{B}} = \nabla\times\tilde{\mathbf{A}} \tag{34}$$

where $\varepsilon^* = \varepsilon - j\sigma/\omega$. The boundary conditions at interface $z = 0$ are the tangential continuity of both the electric and magnetic fields, which amount to the continuities of the following four quantities for the vector potential: $\tilde{\mathbf{A}}_t$, $\tilde{A}_z$, $\partial\tilde{\mathbf{A}}_t/\partial z$, and $\nabla\cdot\tilde{\mathbf{A}}/\varepsilon_r^*$ with $\varepsilon_r^* = \varepsilon^*/\varepsilon_0$. Hence, we have:

$$\mathbf{P}_t = (\mathbf{K}_t^* - \Gamma\mathbf{K}_t) + \mathbf{Q}_t \tag{35}$$

$$\alpha_0 X\mathbf{P}_t = Y(\mathbf{K}_t^* + \Gamma\mathbf{K}_t) - \alpha_1 X\mathbf{Q}_t \tag{36}$$

$$P_z = (K_z^* - \Gamma K_z) + Q_z \tag{37}$$

$$\begin{aligned}\varepsilon_r^*(jk\hat{h}\cdot\mathbf{P}_t + \alpha_0 P_z)X &= (jk\hat{h}\cdot\mathbf{Q}_t - \alpha_1 Q_z)X \\ &\quad + jk\hat{h}\cdot(\mathbf{K}_t^* - \Gamma\mathbf{K}_t)X + (K_z^* + \Gamma K_z)Y\end{aligned} \tag{38}$$

with

$$X = f_1(0) = \frac{e^{-kz_0} - e^{-\alpha_1 z_0}}{\beta_1^2} \tag{39}$$

$$Y = \left.\frac{\partial f_1}{\partial z}\right|_{z=0} = \frac{ke^{-kz_0} - \alpha_1 e^{-\alpha_1 z_0}}{\beta_1^2}. \tag{40}$$

From the above four equations, the coefficients are found to be:

$$\mathbf{P}_t = \frac{Y(\mathbf{K}_t^* + \Gamma\mathbf{K}_t) + \alpha_1 X(\mathbf{K}_t^* - \Gamma\mathbf{K}_t)}{(\alpha_1 + \alpha_0)X} \tag{41}$$

$$\mathbf{Q}_t = \frac{Y(\mathbf{K}_t^* + \Gamma\mathbf{K}_t) - \alpha_0 X(\mathbf{K}_t^* - \Gamma\mathbf{K}_t)}{(\alpha_1 + \alpha_0)X} \tag{42}$$

$$P_z = \frac{jkX(1-\varepsilon_r^*)\hat{h}\cdot\mathbf{P}_t + Y(K_z^* + \Gamma K_z) + \alpha_1 X(K_z^* - \Gamma K_z)}{(\varepsilon_r^*\alpha_0 + \alpha_1)X} \tag{43}$$

$$Q_z = \frac{jkX(1-\varepsilon_r^*)\hat{h}\cdot\mathbf{P}_t + Y(K_z^* + \Gamma K_z) - \varepsilon_r^*\alpha_0 X(K_z^* - \Gamma K_z)}{(\varepsilon_r^*\alpha_0 + \alpha_1)X}. \tag{44}$$

Finally, by substituting (41)-(44) into (33)-(34), the electromagnetic field can be calculated for any given situation. Specifically, in the air, the electric field and magnetic fields are

$$\mathbf{E}_0(\mathbf{r}, t) = \mathrm{Im} \int_{-\pi/2}^{\pi/2} \int_0^{\infty} \mathbf{\Phi}_0 X e^{\alpha_0 z} e^{jk\tilde{\Omega}} k dk d\theta \tag{45}$$

$$\mathbf{B}_0(\mathbf{r}, t) = \mathrm{Im} \int_{-\pi/2}^{\pi/2} \int_0^{\infty} \mathbf{\Psi}_0 X e^{\alpha_0 z} e^{jk\tilde{\Omega}} k dk d\theta \tag{46}$$

with

$$\mathbf{\Phi}_0 = -j\omega\mu_0\mathbf{P} + \frac{jk\hat{h} + \alpha_0\hat{z}}{j\omega\varepsilon_0}(jk\hat{h}\cdot\mathbf{P}_t + \alpha_0 P_z) \tag{47}$$

$$\mathbf{\Psi}_0 = \mu_0(jk\hat{h} + \alpha_0\hat{z})\times\mathbf{P}. \tag{48}$$

In the seawater, the special or primary and the general or secondary solutions of the electromagnetic fields are as follows:

$$\mathbf{E}_1^p(\mathbf{r}, t) = \mathrm{Im} \int_{-\pi/2}^{\pi/2} \int_0^{\infty} \left[-j\omega\mu_0(\bar{\mathbf{K}} f_1 - \mathbf{K}\Gamma f_2) + \mathbf{\Pi}\right] e^{jk\tilde{\Omega}} k dk d\theta \tag{49}$$

$$\begin{aligned}\mathbf{B}_1^p(\mathbf{r}, t) = \mathrm{Im} \int_{-\pi/2}^{\pi/2} \int_0^{\infty} \mu_0 \Big[&(jk\hat{h})\times\left(\bar{\mathbf{K}} f_1 - \mathbf{K}\Gamma f_2\right) \\ &+ \hat{z}\times\left(\bar{\mathbf{K}} f_{1z} - \mathbf{K}\Gamma f_{2z}\right)\Big] e^{jk\tilde{\Omega}} k dk d\theta\end{aligned} \tag{50}$$

$$\mathbf{E}_1^s(\mathbf{r}, t) = \mathrm{Im} \int_{-\pi/2}^{\pi/2} \int_0^{\infty} \mathbf{\Phi}_1 X e^{-\alpha_1 z} e^{jk\tilde{\Omega}} k dk d\theta \tag{51}$$

$$\mathbf{B}_1^s(\mathbf{r}, t) = \mathrm{Im} \int_{-\pi/2}^{\pi/2} \int_0^{\infty} \mathbf{\Psi}_1 X e^{-\alpha_1 z} e^{jk\tilde{\Omega}} k dk d\theta. \tag{52}$$

In the above,

$$\mathbf{\Pi} = \frac{1}{\sigma_1 + j\omega\varepsilon_1}\left\{jk\hat{h}\left[jk\hat{h}\cdot(\bar{\mathbf{K}}f_1 - \mathbf{K}\Gamma f_2) + \hat{z}\cdot(\bar{\mathbf{K}}f_{1z} - \mathbf{K}\Gamma f_{2z})\right] + \hat{z}\left[jk\hat{h}\cdot(\bar{\mathbf{K}}f_{1z} - \mathbf{K}\Gamma f_{2z}) + \hat{z}\cdot(\bar{\mathbf{K}}f_{1zz} - \mathbf{K}\Gamma f_{2zz})\right]\right\} \tag{53}$$

$$f_{1z} = \frac{\partial f_1}{\partial z} = -\mathrm{sgn}(z - z_0)\frac{ke^{-k|z-z_0|} - \alpha_1 e^{-\alpha_1|z-z_0|}}{\beta_1^2} \tag{54}$$

$$f_{2z} = \frac{\partial f_2}{\partial z} = -\frac{ke^{-k(z+z_0)} - \alpha_1 e^{-\alpha_1(z+z_0)}}{\beta_1^2} \tag{55}$$

$$f_{1zz} = \frac{\partial f_{1z}}{\partial z} = \frac{k^2 e^{-k|z-z_0|} - \alpha_1^2 e^{-\alpha_1|z-z_0|}}{\beta_1^2} \tag{56}$$

$$f_{2zz} = \frac{\partial f_{2z}}{\partial z} = \frac{k^2 e^{-k(z+z_0)} - \alpha_1^2 e^{-\alpha_1(z+z_0)}}{\beta_1^2} \tag{57}$$

$$\mathbf{\Phi}_1 = -j\omega\mu_0\mathbf{Q} + \frac{jk\hat{h} - \alpha_1\hat{z}}{\sigma_1 + j\omega\varepsilon_1}(jk\hat{h}\cdot\mathbf{Q}_t - \alpha_1 Q_z) \tag{58}$$

$$\mathbf{\Psi}_1 = \mu_0(jk\hat{h} - \alpha_1\hat{z}) \times \mathbf{Q}. \tag{59}$$

It should be pointed out that the foregoing expressions are not singular when $U\cos\theta \to 0$. Further, the induced magnetic field, actually measured by using a high precision scalar magnetometer is the component of the magnetic field projected along the Earth's magnetic direction, i.e.,

$$S(\mathbf{r}, t) = \frac{\mathbf{F}_0}{|\mathbf{F}_0|}\cdot\mathbf{B}(\mathbf{r}, t) \tag{60}$$

IV. SIMULATION RESULTS

In this Section, all the integrals (45)-(46) and (49)-(52), which take the same form, are evaluated numerically:

$$\mathbf{M}(\mathbf{r}, t) = \int_{-\pi/2}^{\pi/2} d\theta \int_0^{\infty} \mathbf{N}(k, \theta, z)e^{jk\tilde{\Omega}}dk. \tag{61}$$

The electric field or magnetic field is extracted by taking the imaginary part of $\mathbf{M}(\mathbf{r}, t)$, after inserting appropriate $\mathbf{N}(k, \theta, z)$. Equation (16) shows that the integrand $\mathbf{N}(k, \theta, z)$ has a single polar point at $k = k_p = k_0\sec^2\theta$. So, the integral routine for k can be taken to be the same as in Figure 2, and the integral with respect to k can be written as

$$\begin{aligned}\int_0^{\infty} &\mathbf{N}(k, \theta, z)e^{jk\tilde{\Omega}}dk \\ &= (j2\pi)\lim_{k\to k_p}\left[(k - k_p)\mathbf{N}(k, \theta, z)e^{jk\tilde{\Omega}}\right] \\ &\quad + (1 + j)\int_0^{\infty} d\eta\left[\mathbf{N}(k, \theta, z)e^{jk\tilde{\Omega}}\right]_{k=(1+j)\eta}\end{aligned} \tag{62}$$

for $\tilde{\Omega} = (x + Ut)\cos\theta + y\sin\theta > 0$, and

$$\int_0^{\infty} \mathbf{N}(k, \theta, z)e^{jk\tilde{\Omega}}dk = (1 - j)\int_0^{\infty} d\eta\left[\mathbf{N}(k, \theta, z)e^{jk\tilde{\Omega}}\right]_{k=(1-j)\eta} \tag{63}$$

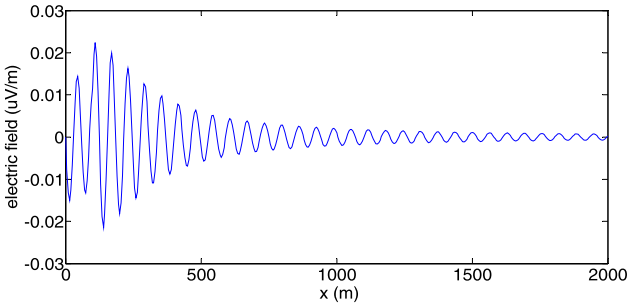

FIGURE 6. Electric field's y-component at 30m above the sea surface, ascribed to the free surface Kelvin wake.

for $\tilde{\Omega} \le 0$. As a result, $\mathbf{M}(\mathbf{r}, t) = \mathbf{M}_1(\mathbf{r}, t) + \mathbf{M}_2(\mathbf{r}, t)$ is written with

$$\mathbf{M}_1(\mathbf{r}, t) = (j2\pi)\int_{-\pi/2}^{\pi/2} d\theta\, u(\tilde{\Omega})\lim_{k\to k_p}\left[(k - k_p)\mathbf{N}(k, \theta, z)e^{jk\tilde{\Omega}}\right] \tag{64}$$

$$\begin{aligned}\mathbf{M}_2(\mathbf{r}, t) = &\int_{-\pi/2}^{\pi/2} d\theta\left\{u(\tilde{\Omega})(1 + j)\int_0^{\infty} d\eta\left[\mathbf{N}(k, \theta, z)e^{jk\tilde{\Omega}}\right]_{k=(1+j)\eta}\right. \\ &\left. + \left[1 - u(\tilde{\Omega})\right](1 - j)\int_0^{\infty} d\eta\left[\mathbf{N}(k, \theta, z)e^{jk\tilde{\Omega}}\right]_{k=(1-j)\eta}\right\}\end{aligned} \tag{65}$$

in which the step function $u(\tilde{\Omega})$ is defined the same way as (10). $\mathbf{M}_1(\mathbf{r}, t)$ is obviously the contribution from the free surface Kelvin wake, and $\mathbf{M}_2(\mathbf{r}, t)$ from the localized volume wake near the moving body.

The following simulation parameters are taken: $L = 100$m, $V = 4\pi \times 10^4\text{m}^3$, $z_0 = 50$m, $U = 10$m/s, $\sigma_1 = 5$S/m, and $\varepsilon_1 = 80\varepsilon_0$. The Earth's magnetic field is taken to be $|\mathbf{F}_0| = 5 \times 10^4$ nT, and $\mathbf{F}_0/|\mathbf{F}_0| = (\frac{1}{2}, 0, \frac{\sqrt{3}}{2})$ or $(0, -\frac{1}{2}, \frac{\sqrt{3}}{2})$ for the body moving toward the north or toward the west, respectively.

First, the part ascribed to the surface Kelvin wake, i.e. the results given by (64), is considered. The distribution of the produced electric field along the centerline at 30 m above the sea surface is plotted in Figure 6, which shows that the maximum magnitude is about 0.02 μV/m. The produced magnetic anomaly field, calculated by (60), at 30 m above the sea surface is plotted in Figure 7, which shows that the maximum magnitude is about 13 pT. The spectrum of Figure 7(a) is shown in Figure 8. It can be seen that, because the fundamental spatial frequency of the oscillating magnetic anomaly field is $k = k_0 = g/U^2 = 0.0981$, the time frequency is $\omega = k_0 U$ or $f = k_0 U/2\pi = 0.156$ Hz. This implies that a stationary scalar magnetometer in the air will record a dying oscillating magnetic anomaly field, with oscillating frequency at 0.156 Hz. It should be noted that the oscillation is a direct reflection of the Kelvin wake of water

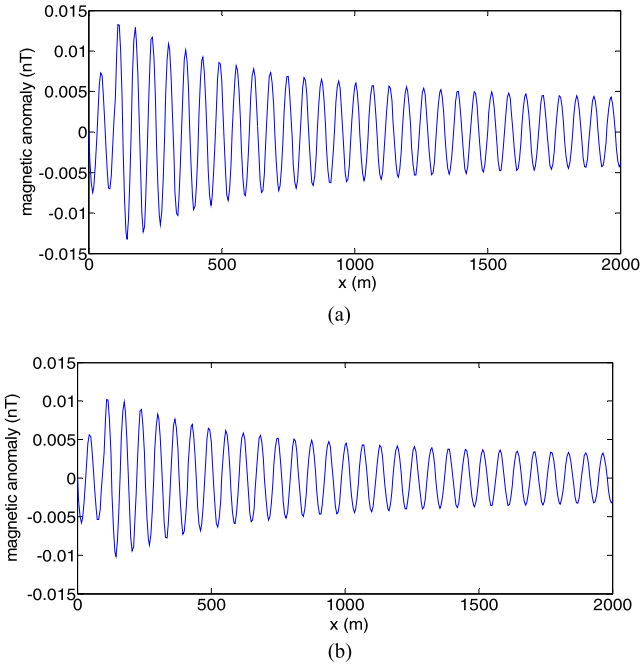

FIGURE 7. Magnetic anomaly fields at 30m above the sea surface, ascribed to the free surface Kelvin wake for the body moving (a) toward the north, and (b) toward the west.

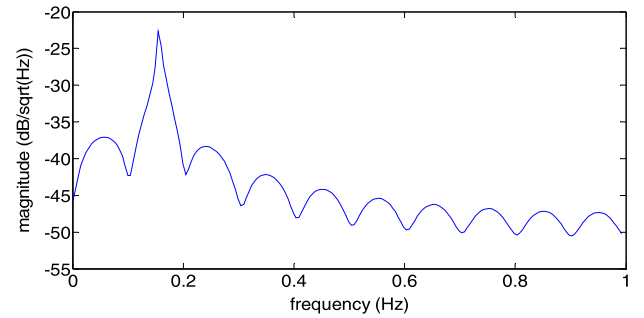

FIGURE 8. Spectrum of the magnetic anomaly fields shown in Figure 7(a), where 0 dB = 1 nT/$\sqrt{\text{Hz}}$.

wave, and not of the electromagnetic wave. The wavelength of the water wave is $\lambda_w = 2\pi/k_0 \approx 64$m, while that of the electromagnetic wave is

$$\lambda_{em} = 2\pi \frac{c}{\omega} = \frac{c}{U}\lambda_w. \tag{66}$$

where $c \approx 3 \times 10^8$ m/s is the speed of light in free space.

In the seawater, the electric field's y-component and the magnetic anomaly field produced at 30 m below the sea surface are shown in Figure 9 and Figure 10. By comparing them with Figure 6 and Figure 7, it is seen that the fields produced in the seawater are much stronger because of partial contribution directly by the electric currents in the medium.

The distribution pattern of magnetic anomaly field near the sea surface is that of a two-dimensional (2D) magnetic wake, as shown in Figure 11. It is seen that the maximum magnitude is about 0.3 nT, and the same can be regarded as

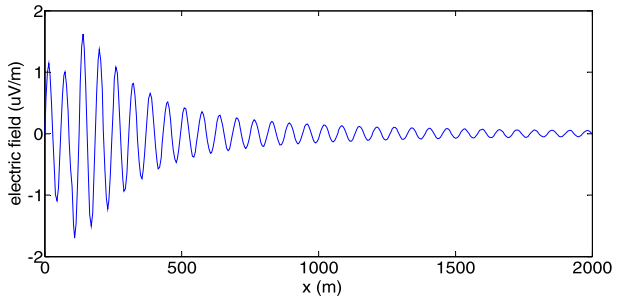

FIGURE 9. Electric field's y-component at 30m below the sea surface, ascribed to the free surface Kelvin wake.

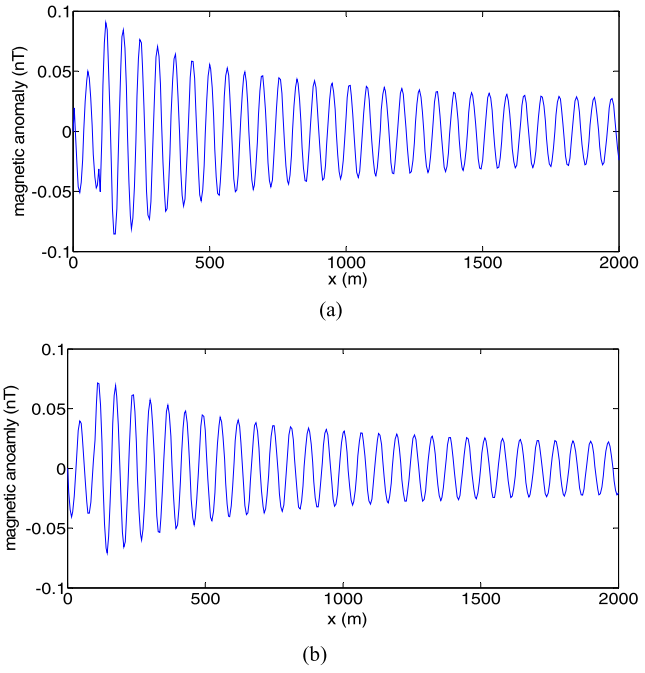

FIGURE 10. Magnetic anomaly fields at 30m below the sea surface, ascribed to the free surface Kelvin wake for the body moving (a) toward the north, and (b) toward the west.

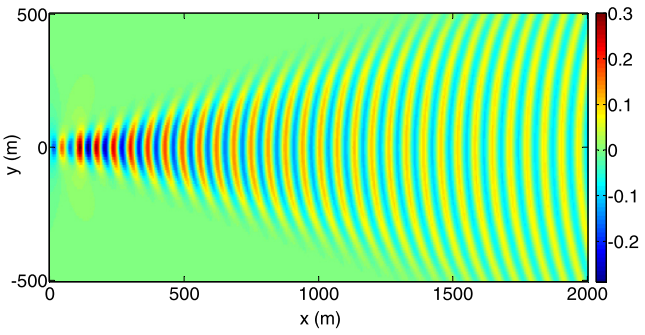

FIGURE 11. Magnetic anomaly pattern over the sea surface, ascribed to the free surface Kelvin wake.

a big value, considering the precision of commercial optical pumping atomic magnetometer, which is typically a few pT.

Next, the part that is largely ascribed to the volume wake, i.e., the results given by (65), is considered. As before,

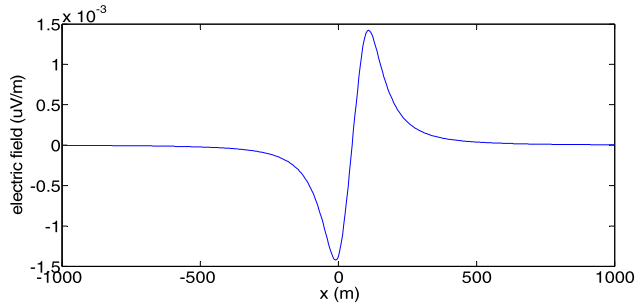

FIGURE 12. Electric field's y-component at 30m above the sea surface, ascribed to the volume wake.

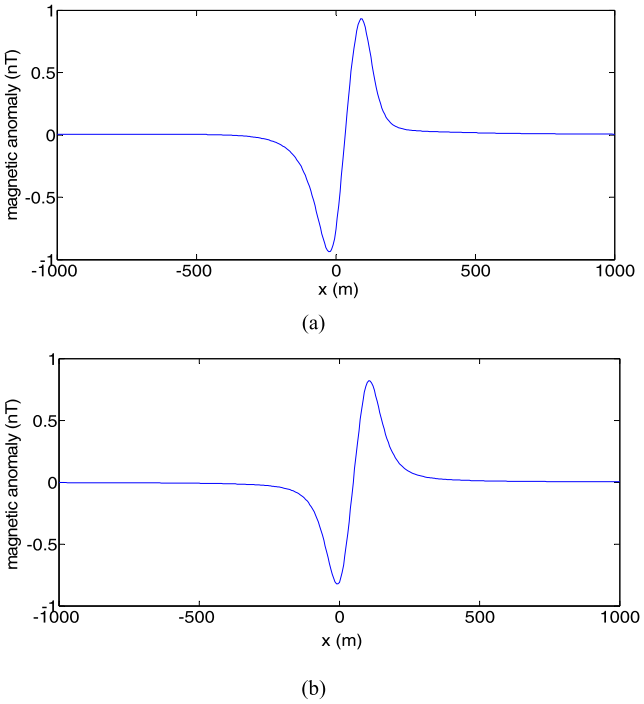

FIGURE 13. Magnetic anomaly fields at 30m above the sea surface, ascribed to the volume wake for the body moving (a) toward the north, and (b) toward the west.

the electromagnetic fields at 30 m above the sea surface and 30 m below the sea surface are calculated. The results corresponding to Figure 6 through Figure 11 are shown in Figure 12 through Figure 17. In the air, the electric field ascribed to the volume wake is much weaker than that ascribed to the surface Kelvin wake; however, the magnetic anomaly field ascribed to the volume wake is much stronger than that ascribed to the surface Kelvin wake. By comparing Figure 7 with Figure 13, and Figure 8 with Figure 14, it can be seen that the former is an attenuating oscillation or a narrowband signal, while the latter is a bipolar pulse or a wideband signal. The 2D magnetic anomaly pattern ascribed to the volume wake, shown in Figure 17, is highly localized, unlike the one shown in Figure 11, but the magnitude is greater by several times.

Finally, the attenuating characteristics of the magnetic anomaly fields are examined in the elevation direction.

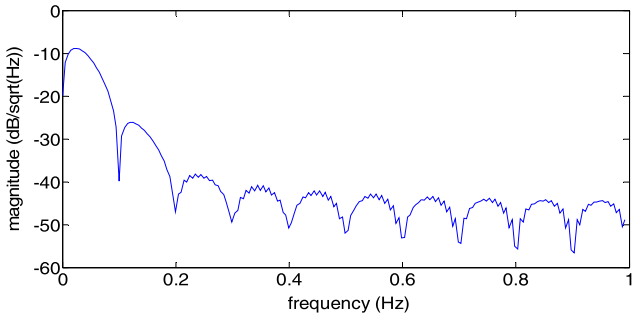

FIGURE 14. Spectrum of the magnetic anomaly fields shown in Figure 13(a), where $0\ \text{dB} = 1\ \text{nT}/\sqrt{\text{Hz}}$.

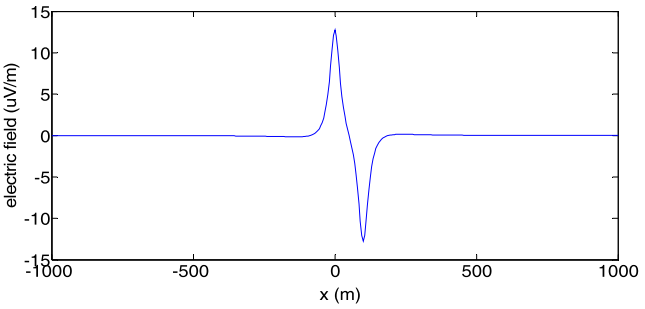

FIGURE 15. Electric field's y-component at 30m below the sea surface, ascribed to the volume wake.

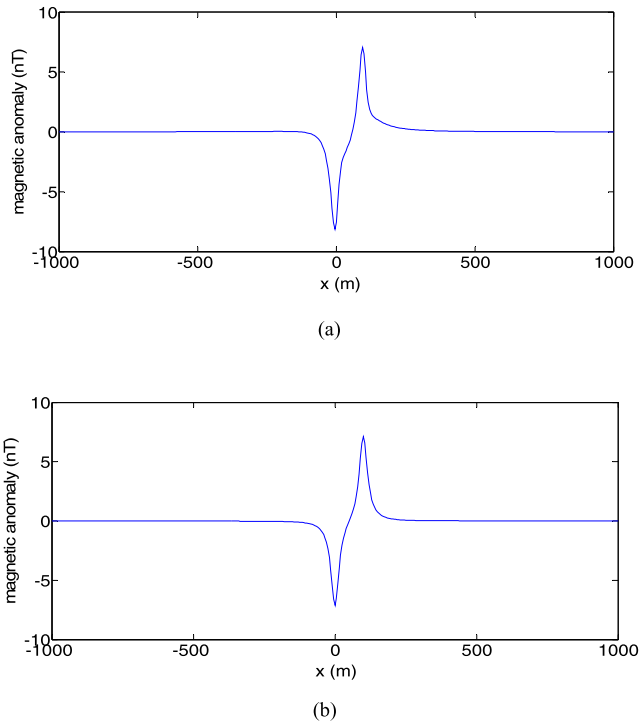

FIGURE 16. Magnetic anomaly fields at 30m below the sea surface, ascribed to the volume wake for the bodies moving toward (a) north and (b) west.

The fields along a vertical line that passes through the point $(x, y) = (140, 0)$ m are computed and the results are shown in Figure 18. For the part ascribed to the surface Kelvin

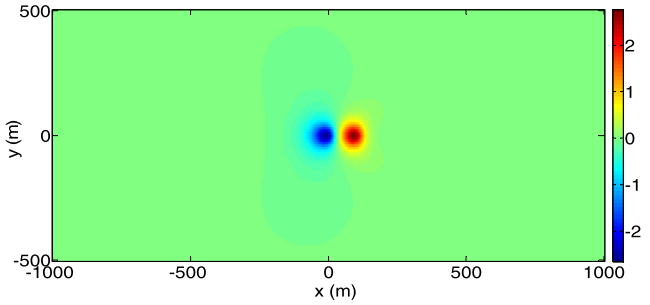

FIGURE 17. Magnetic anomaly pattern over the sea surface, ascribed to the volume wake.

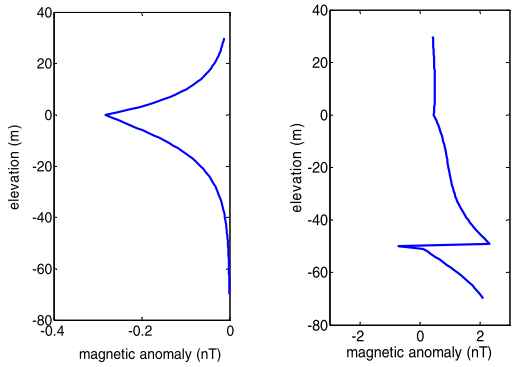

FIGURE 18. Magnetic anomaly fields along a vertical line passing through the point $(x, y) = (140, 0)$ m. (a) The part ascribed to surface Kelvin wake, and (b) the part ascribed to volume wake.

wake, the magnetic anomaly field has the maximum magnitude of 0.3 nT near the sea surface, which attenuates non-symmetrically in the air and seawater. The attenuation in the seawater region is slower because of partial contribution directly by the electric currents. For the part ascribed to the volume wake, the maximum magnitude is attained near 50 m below the sea surface, where the two Havelock point sources are situated. A sharp change is noticed at the depth (50 m), which may be accounted for by the reversal of the vertical component of the wake seawater flow at the depth.

V. CONCLUDING REMARKS

Evaluation of electromagnetic fields produced by the wake of underwater moving bodies holds great potential value for both civil and military applications. Moving seawater can induce weak electric currents in the medium by cutting the Earth's magnetic field, which may produce detectable electromagnetic fields near or under the sea surface.

To find the electric currents in the seawater, the velocity field of the wake has to be modelled first. After linearizing the nonlinear kinematics and kinetics equations at the air-seawater interface, a slender body moving under the sea surface is considered, treating it as a pair of Havelock point sources. The wake of the moving body includes two distinct parts: the surface Kelvin wake and the volume wake. The surface Kelvin wake is an attenuating oscillation that is restricted mainly to a V-shape area of 39 degrees, and it can spread over several kilometers and sustain more than ten minutes. The volume wake is largely localized near the body and moves along with the body.

The electromagnetic fields produced by the wake are also composed of two distinct parts. The part ascribed to the surface Kelvin wake is an attenuating oscillation and exists only on the rear side of body, which is a direct reflection of the surface wake itself. However, it should not be interpreted that the electric currents carried by the surface Kelvin wake produce only this part of electromagnetic fields, because the partial fields do not meet the boundary conditions. In fact, the electric currents carried by the surface Kelvin wake also produce highly damping fields on both the front and rear sides of body. The part of electromagnetic fields, ascribed to the volume wake, is largely localized to the body and moves along with the body, just like the wake itself. Again, it should not be interpreted that the electric currents carried by the volume wake produce all this part of electromagnetic fields, because the partial electromagnetic fields do not meet boundary conditions, either. In fact, this part includes the monotonically damping ingredients produced by the electric currents carried by the surface Kelvin wake.

The part of electromagnetic fields that is ascribed to the surface Kelvin wake is an attenuating oscillation, which can be seen as a steady narrowband signal, while the part ascribed to the volume wake is a bipolar pulse, which can be seen as a wideband signal. Therefore, separating these two parts of signals seems to be feasible, which provides an additional feature for probing the body.

Finally, it is to be noted that the authors employ a non-stratified, infinite depth ocean model for the present study. But, in future, for feasibility studies of practical applications, stratified and finite depth configuration should be considered. Moreover, the present work employs a slender body, which is treated as a pair of Havelock point sources. But, for a more accurate evaluation or for non-slender bodies, a fully numerical method will have to be developed to solve both the velocity fields and electromagnetic fields.

REFERENCES

[1] M. Faraday, "The Bakerian lecture: Experimental researches in electricity, Second Series," *Phil. Trans. Roy. Soc. London*, vol. 122, pp. 163–194, Jan. 1832.

[2] F. B. Young, H. Gerrard, and W. Jevons, "On electrical disturbances due to tides and waves," *J. Phil. Mag. Ser.*, vol. 6, no. 40, pp. 149–159, 1920.

[3] K. C. Maclure, R. A. Hafer, and J. T. Weaver, "Magnetic variations produced by ocean swell," *Nature*, vol. 204, pp. 1290–1291, Dec. 1964.

[4] D. C. Fraser, "Magnetic field of ocean waves," *Nature*, vol. 206, pp. 605–606, Mar. 1965.

[5] J. T. Weaver, "Magnetic variations associated with ocean waves and swell," *J. Geophys. Res.*, vol. 70, pp. 1921–1929, Apr. 1965.

[6] S. V. Semkin and V. P. Smagin, "The effects of self-induction on magnetic field generated by sea surface waves," *Atmos. Ocean. Phys.*, vol. 48, pp. 207–213, Feb. 2012.

[7] W. Podney and R. Sager, "Measurement of fluctuating magnetic gradients originating from oceanic internal waves," *Science*, vol. 205, pp. 1381–1382, Sep. 1979.

[8] H. T. Beal and J. T. Weaver, "Calculations of magnetic variations induced by internal ocean waves," *J. Geophys. Res.*, vol. 75, no. 33, pp. 6846–6852, 1970.

[9] A. D. Chave, "On the electromagnetic fields induced by oceanic internal waves," *J. Geophys. Res.*, vol. 89, no. C6, pp. 10519–10528, 1984.

[10] K. M. Bhatt, A. Hordt, P. Weidelt, and T. Hanstein, "Motionally induced electromagnetic field within the ocean," in *Proc. 23th Schmucker-Weidelt-Kolloquium Elektromagnetische Tiefenforschung, Heimvolkshochschule Seddiner See*, Sep./Oct. 2009, pp. 46–59.

[11] J. Saynisch, J. Peterelt, C. Irrgang, and M. Thomas, "Impact of oceanic warming on electromagnetic oceanic tidal signals: A CMIP5 climate model-based sensitivity study," *Geophys. Res. Lett.*, vol. 44, pp. 4994–5000, May 2017.

[12] B. L. Wang and H. Liu, "Space-time behavior of magnetic anomalies induced by tsunami waves in open ocean," *Proc. Roy. Soc. A*, vol. 469, no. 2157, p. 20130038, May 2013.

[13] N. Zou and A. Nehorai, "Detection of ship wakes using an airborne magnetic transducer," *IEEE Trans. Geosci. Remote Sens.*, vol. 38, no. 1, pp. 532–539, Jan. 2000.

[14] O. Yaakobi, G. Zilman, and T. Miloh, "Detection of the electromagnetic field induced by the wake of a ship moving in a moderate sea state of finite depth," *J. Eng. Math.*, vol. 70, pp. 17–27, Jul. 2011.

[15] D. Madurasinghe, "Induced electromagnetic fields associated with large ship wakes," *Wave Motion*, vol. 20, no. 2, pp. 283–292, 1994.

[16] D. Madurasinghe and E. O. Tuck, "The induced electromagnetic field associated with submerged moving bodies in an unstratified conducting fluid," *IEEE J. Ocean. Eng.*, vol. 19, no. 2, pp. 193–199, Apr. 1994.

[17] X. J. Zhu and M. Y. Xia, "Magnetic field induced by wake of moving body in wind waves," *Progr. Electromagn. Res.*, vol. 149, pp. 109–118, Oct. 2014.

[18] Z. H. Xu, C. P. Du, and M. Y. Xia, "Modeling of electromagnetic fields induced by moving seawater due to an undersea vehicle," in *Proc. IEEE Interfaces Conf. Comput. Electromagn.*, Kumamoto, Japan, Mar. 2017, pp. 72–74.

[19] J. H. Filloux, "Techniques and instrumentation for study of natural electromagnetic induction at sea," *Phys. Earth Planetary Interiors*, vol. 7, pp. 323–338, Sep. 1973.

[20] T. B. Sanford, "Florida current volume transports from voltage measurements," *Science*, vol. 227, pp. 302–304, Jan. 1985.

[21] M. A. Fallah and H. Abiri, "Multi-sensor approach in vessel magnetic wake imaging," *Wave Motion*, vol. 51, pp. 60–76, Jan. 2014.

[22] C. S. Cox *et al.*, "Controlled source electromagnetic sounding of the oceanic lithosphere," *Nature*, vol. 320, no. 1, pp. 52–54, 1986.

[23] S. Constable, "Review paper: Instrumentation for marine magnetotelluric and controlled source electromagnetic sounding," *Geophys. Prospecting*, vol. 61, pp. 505–532, Jun. 2013.

[24] J. Newman, *Marine Hydrodynamics*. Cambridge, MA, USA: MIT Press, 1977.

[25] T. Gourlay and E. Dawson, "A havelock-source panel method for near-surface submarines," *J. Marine Sci. Appl.*, vol. 14, no. 3, pp. 215–224, 2015.

[26] R. W. Yeung and T. C. Nguyen, "Waves generated by a moving source in a two-layer ocean of finite depth," *J. Eng. Math.*, vol. 35, nos. 1–2, pp. 85–107, 1999.

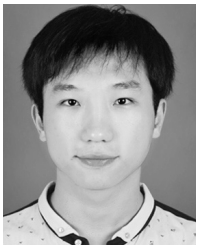

ZHIHUA XU (S'16) received the B.S. degree in communication engineering from the University of Science and Technology of Beijing, Beijing, China, in 2015. He is currently pursuing the Ph.D. degree with the School of Electronics Engineering and Computer Science, Peking University, Beijing. His research interests are electromagnetic field theory and applications, such as marine electromagnetics and magnetic anomaly detection.

CHANGPING DU (S'16) received the master's degree in electronic engineering from the University of Electronic Science and Technology of China, Chengdu, China, in 2015. He is currently pursuing the Ph.D. degree with the School of Electronics Engineering and Computer Science, Peking University, Beijing, China. His research interests include electromagnetic modeling and surveying, especially obscured ferromagnetic objects and pertinent signal processing techniques.

MINGYAO XIA (M'00–SM'03) received the master's and Ph.D. degrees in electrical engineering from the Institute of Electronics, Chinese Academy of Sciences (IECAS), in 1988 and 1999, respectively. From 1988 to 2002, he was with IECAS as an Engineer and a Senior Engineer. He was a Visiting Scholar at the University of Oxford, U.K., from 1995 to 1996. From 1999 to 2000 and from 2002 to 2002, he was a Senior Research Assistant and a Research Fellow, respectively, with the City University of Hong Kong. He joined Peking University as an Associate Professor in 2002 and was promoted to Full Professor in 2004. He moved to the University of Electronic Science and Technology of China as a Chang-Jiang Professor nominated by the Ministry of Education of China in 2010. He returned to Peking University after finishing the appointment in 2013. His research interests include electromagnetic theory, numerical methods and applications, such as wave propagation and scattering, electromagnetic imaging and probing, microwave remote sensing, antennas, and microwave components. He was a recipient of the Young Scientist Award of the URSI in 1993. He was awarded the first-class prize on Natural Science by the Chinese Academy of Sciences in 2001. He was a recipient of the Foundation for Outstanding Young Investigators presented by the National Science Foundation of China in 2008. He served as an Associate Editor for the IEEE TRANSACTIONS ON ANTENNAS AND PROPAGATION.